

Supporting information

Optimum Nanoparticles for Electrocatalytic Oxygen Reduction: The Size, Shape and New Design

Guang-Feng Wei, Zhi-Pan Liu*

Shanghai Key Laboratory of Molecular Catalysis and Innovative Materials, Department of Chemistry, Key Laboratory of Computational Physical Science (Ministry of Education), Fudan University, Shanghai 200433, China

Part I Derivation of the realistic total surface energy G_{sur}^r of nanoparticles

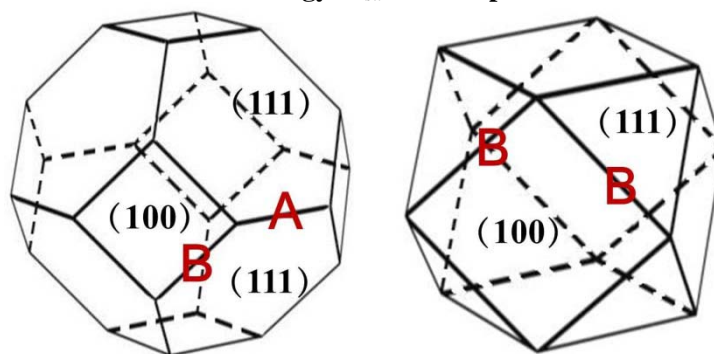


Fig. S1 The perspective of truncated octahedron (left) and cuboctahedron (right).

Table S1 The calculated surface free energy data and their geometrical parameters of three selected Pt nanoparticles in aqueous solution (via CM-MPB model). These data are utilized in the fitting to obtain eq S7.

	G_{sur}^r (eV)	G_{sur}^i (eV)	ΔG (eV)	A (Å)	B (Å)
Pt₂₀₁	113.88	74.84	39.04	5.63	5.63
Pt₂₆₀	139.90	95.35	44.55	2.81	8.44
Pt₄₀₅	177.66	129.58	48.08	5.63	8.44

For large particles where the Wulff construction rule can be applied correctly, the shape is controlled by the surface energy, expressed as eq S1 (Wulff, G., *Z Krystallogr. Mineral* **1901**, 34, 449.) Given the particle in a truncated octahedron shape, we can use eq S2 to compute the $D_{(100)}$: $D_{(111)}$ ratio.

$$D_{(100)} : D_{(111)} = \gamma_{\{100\}} : \gamma_{\{111\}} \quad (\text{S1})$$

$$S = D_{(100)} / D_{(111)} = [1 - B/(A+2B)] \cdot \sqrt{3} \quad (\text{S2})$$

Where A and B are the length of the (111)-(111) edge and (1111)-(100) edge, respectively (see S-Fig.1). Using the periodic DFT/CM-MPB approach, we have computed the surface energy (γ) of {100} and {111} in aqueous solution, which are 10.55 and 8.32 eV/nm², respectively. This yields an equilibrium $S(D_{(100)}: D_{(111)})$ being 1.27 in aqueous solution. Eq. S3 from the Wulff construction rule is in principle only valid for very large particles. The presence of the edges and corners in real nanoparticles is expected to affect the surface energy and in turn changes the equilibrium shape. To take into account of this effect and to predict more realistic S values for nanoparticles, we have carried out the following analysis based on the DFT energetics of the computed anatase particles. First, the ideal surface free energy (G_{sur}^i) of a truncated octahedron particle is expressed as eq S3, which can be computed simply from the surface energy of extended surfaces $\gamma_{(100)}$ and $\gamma_{(111)}$ without considering the edge/corner effects. To obtain a realistic value (G_{sur}^f) for nanoparticles, a correction term ΔG (due to the presence of edge/corners) must be amended, as in eq S4.

$$G_{\text{sur}}^i = 2\sqrt{3}[(A+2B)^2 - 3B^2] \cdot \gamma_{(111)} + 6B^2 \cdot \gamma_{(100)} \quad (\text{S3})$$

$$G_{\text{sur}}^r = G_{\text{sur}}^i + \Delta G \quad (\text{S4})$$

$$G_{\text{sur}}^r = G_{\text{NP}} - x \cdot G_{\text{H}_2\text{O}} - n \cdot G_{\text{bulk}} \quad (\text{S5})$$

Next, from DFT energetics of the calculated nanoparticles in aqueous solution, we are able to calculate the G_{sur}^f using eq S5, where the $G_{\text{NP}/\text{H}_2\text{O}/\text{bulk}}$ is the free energy of nanoparticle/H₂O/bulk Pt, and x and n account for the total number of the dissociated H₂O on the nanoparticle and the Pt atom, respectively. By utilizing eqs S3-5, ΔG of three selected nanoparticles (i.e., Pt₂₀₁; Pt₂₆₀ and Pt₄₀₅) have been computed as listed in S-Table 1. According to the shape of the truncated octahedron nanoparticles, we can approximately attribute the origin of ΔG to a fixed number of edges and corners in the nanoparticle, which can be written as

$$\Delta G = 12A \cdot \gamma_{(\text{edge-A})} + 24B \cdot \gamma_{(\text{edge-B})} + \gamma_{\text{cor}} \quad (\text{S6})$$

where A/B is the edge length as defined in Fig. S1, $\gamma_{(\text{edge-A/B})}$ is the free energy correction associated with the edge A/B, and γ_{cor} is the free energy correction due to the corners. By fitting the ΔG data in S-Table 1, with eq S6, we can deduced the value of $\gamma_{(\text{edge-A/B})}$ ($\gamma_{(\text{edge-A})} = 10.43$ eV/Å, $\gamma_{(\text{edge-B})} = 13.38$ eV/Å) and then finally arrived at a formula, eq S7, to predict G_{sur}^f , where 1.2520, 3.2100, and 13.9315 are the fitted values (the unit for A/B is Å and for G_{sur}^f is eV).

$$G_{\text{sur}}^r = 0.2883 \cdot A^2 + 0.9215 \cdot B^2 + 1.1530 \cdot AB + 1.2520 \cdot A + 3.2100 \cdot B + 13.9315 \quad (\text{S7})$$

Based on eq S7, we can finally predict the equilibrium shape of nanoparticles by minimizing G_{sur}^f at a given volume V ($V = \sqrt{2/3} \cdot [(A+2B)^3 - 3B^3]$) with the Lagrange multiplier method. Starting from fitted equation eq S7, we utilize Lagrange multiplier method to derive the relationship between $S [= \sqrt{3} \cdot (1 - B/(A+2B))]$ and A under the constraint of the fixed volume V, which defines

$$L(A, B, \lambda) = G_{\text{sur}}(A, B) + \lambda \cdot (V(A, B) - V) \quad (\text{S8})$$

To get the minimum of $L(A, B, \lambda)$, the grads of L should satisfy the following equations:

$$\partial L / \partial A = \partial G_{\text{sur}} / \partial A + \lambda \cdot \partial V / \partial A = 0 \quad (\text{S9})$$

$$\partial L / \partial B = \partial G_{\text{sur}} / \partial B + \lambda \cdot \partial V / \partial B = 0 \quad (\text{S10})$$

$$\partial L / \partial \lambda = V(A, B) - V = 0 \quad (\text{S11})$$

We can solve eq S9-11 at a pre-defined V, and calculate the A and B values, through which S is obtained. By changing V, we finally can get the curve for S versus $D_{(111)}$ ($D_{(111)} = \sqrt{6/3} \cdot (A+2B)$), as shown in Fig. 1a in the main text.

Part II Surface phase diagram of Pt nanoparticle

Theoretically, the thermodynamic equilibrium O coverage under electrochemical potentials can be determined by constructing the surface phase diagram.¹⁻³ Detailed calculation setups for constructing the surface phase diagram have been described in our recent study.^{3,4} The effect of the water environment on the phase diagram and on the reaction kinetics has been examined through a continuum solvation model with a smooth dielectric function by solving the Poisson-Boltzmann equation numerically in the periodic slab as implemented recently.⁵⁻⁸

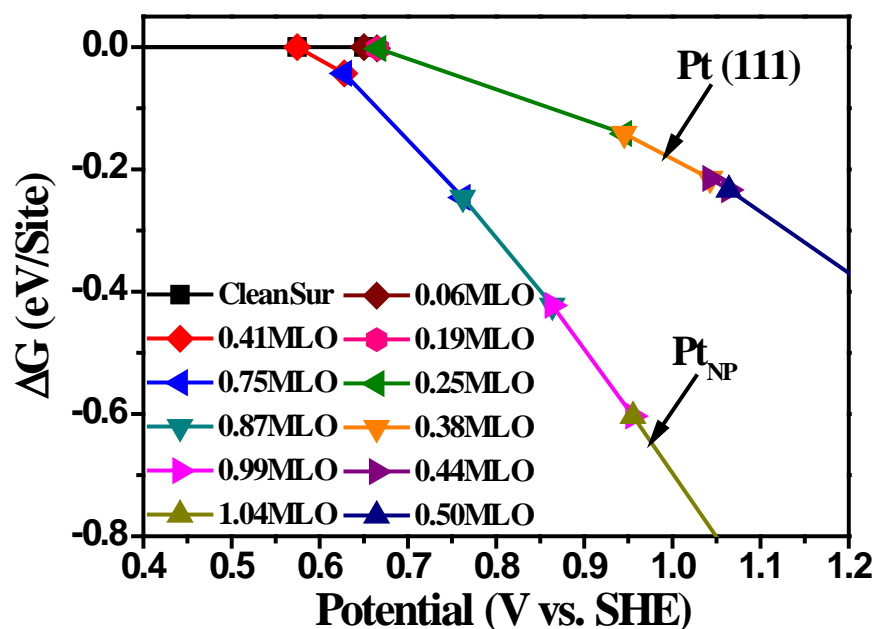


Fig. S2 The surface phase diagram of Pt₂₂₁ nanoparticle (Pt_{NP}) and Pt(111). The apparent oxygen coverage ($N_{\text{Oad}}/N_{\text{Ptsur}}$) of Pt₂₂₁ is much higher than that on Pt(111) surface.

At ORR steady state, the surface stays at a constant condition as dictated by the chemical potentials of reactant O₂ (gas phase), H₂O (solution) and acid (H⁺, solute) under a certain electrochemical potential. To address the steady state kinetics, it is essential to know the in situ O coverage on the surface that can affect the kinetics of reactions significantly. Kinetically, this can be done by evaluating quantitatively the free energy barrier (ΔG_a) for the O-atom generation and the O-atom removal over various O-covered Pt nanoparticle surfaces at a concerned potential. ΔG_a of these two processes have to be comparable at the steady state. For the purpose of a fast screening, we first represent the O atom generation and removal processes by the O₂ direct dissociation (O₂→2O) and the O atom reduction to OH (O + H⁺ + e⁻→OH) reactions, respectively. By this way, the potential effect on the overall reaction is taken into account by considering the free energy stability of the final product H₂O with respect to the reactant O₂ and the ΔG_a of the O removal (O₂ dissociation kinetics is not potential dependent as no explicit electron transfer involves). The O coverage estimated could then be validated by performing a complete reaction pathway searching and kinetics analysis.

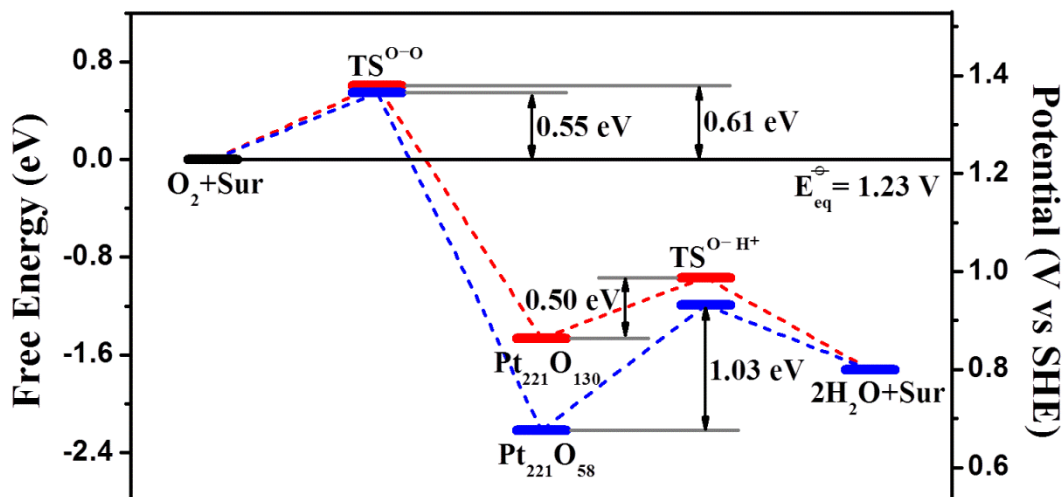


Fig. S3 The steady-state kinetics analysis for determining the surface O coverage of Pt_{221} .

Here is an example for the steady state analysis of the O coverage on Pt_{221} nanoparticle. As shown in Fig. S3 (the electrochemical potential is set at 0.8 V for illustration), O_2 dissociation into atomic O on Pt_{221} at both 0.41 ML and 0.93 ML O coverage (refer to $Pt_{221}O_{56}$ and $Pt_{221}O_{128}$) are a highly exothermic process (by $>1.2\text{eV}$ in ΔG) and have similar reaction barriers (ΔG_a equals to 0.55 eV and 0.61 eV, respectively). On the other hand, the subsequent reduction of O atoms on the $Pt_{221}O_{58}$ surface to restore the 0.41 ML O is kinetically more difficult with the overall ΔG_a being 1.03 eV at 0.8 V. This indicates that the surface O atom coverage will build up to reach a higher O coverage. In contrast, the O_2 dissociation becomes increasingly difficult for O coverages above 0.99 ML due to few surface Pt sites on nanoparticle surface for O_2 adsorption. Once the O coverage is at or above 0.99 ML, the removal of the additional surface O atoms will be kinetically much faster than the uptake of the surface O atoms. Obviously, because of the large gap in ΔG_a for reactions occurring below and above 0.93 ML O covered surface, a steady state surface O coverage in between 0.93~0.99 ML is generally the most favorable for ORR on Pt(111) over a potential range, i.e. from 0.8 to 1.0 V from Fig. S3. A 0.93 ML O coverage is therefore identified as the low limit for the surface O coverage and hereafter utilized as the initial surface O coverage for investigating the ORR kinetics on Pt_{221} .

Part III Pt nanoparticles under electrochemical conditions and ORR activity

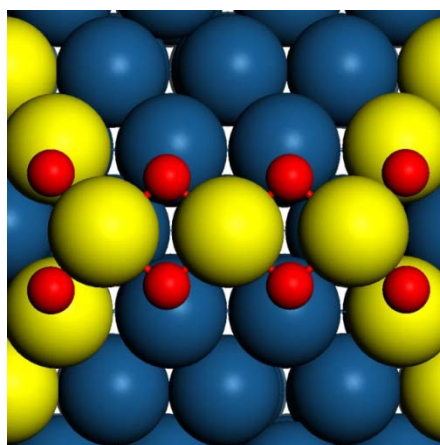


Fig. S4 The enlarged view of edge-A of Pt₄₀₅ nanoparticle at 0.65 V. Large blue ball: terrace Pt; large yellow ball: edge Pt; red ball: O.

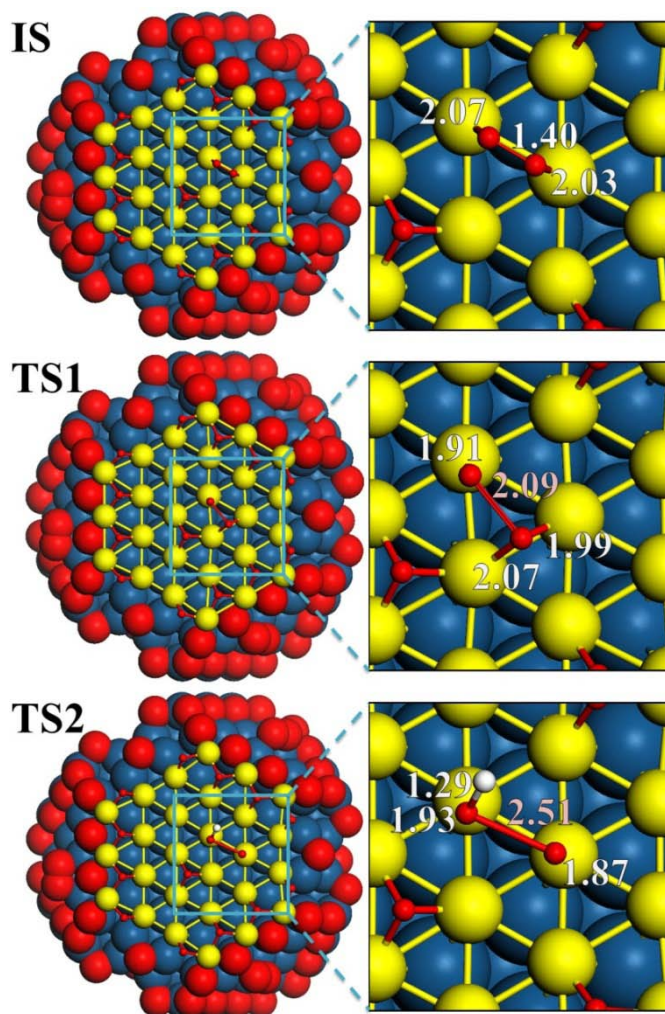


Fig. S5 The most stable surface structures of IS and TS of O-O direct dissociation (TS1) and O-OH dissociation (TS2) on Pt₂₈₈ with the presence of adsorbed atomic oxygen at 0.9 V vs RHE. The nearby solvated proton [H₇O₃⁺] that can stabilize the IS and TSs is not shown for clarity. Large blue ball and yellow ball: Pt; red ball: O; small white ball: H.

Part IV Au-framed Pt nanoparticles

Exchange Atom	ΔG (eV)
A1 \leftrightarrow P1	0.18
A1 \leftrightarrow P2	0.12
A2 \leftrightarrow P1	0.26
A2 \leftrightarrow P2	0.36
A2 \leftrightarrow P3	0.20
A3 \leftrightarrow P1	0.14
A3 \leftrightarrow P2	0.19
A3 \leftrightarrow P3	0.08

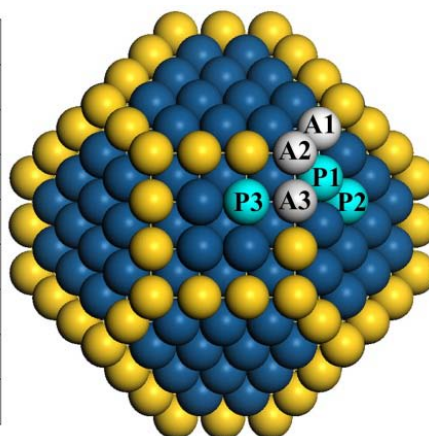


Fig. S6 The energy difference for swapping surface Pt atoms with the edge Au atoms in the Au-framed particle (positive means energy cost for moving the edged Au to the terrace). A1, A2, and A3 represents Au atoms; P1, P2 and P3 represents Pt atoms. The results suggest that the Au-framed structure (with all edges being occupied by Au atoms) is the most stable surface pattern.

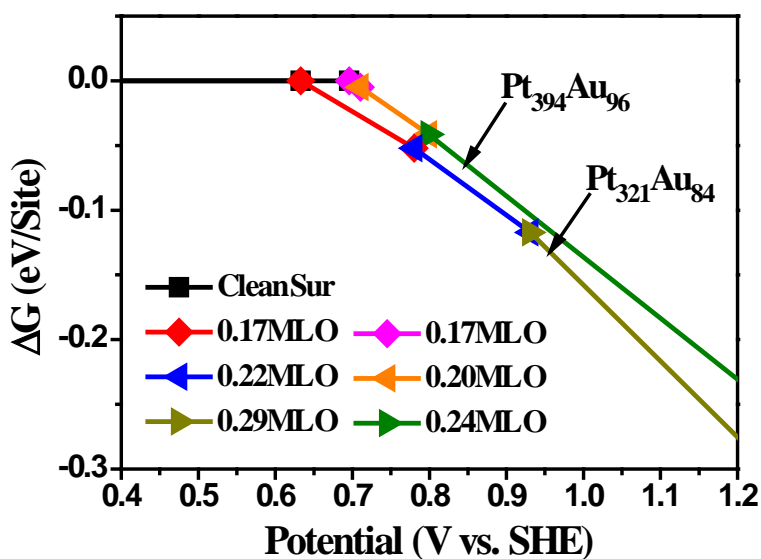


Fig. S7 The surface phase diagram of Au-framed Pt nanoparticles ($\text{Pt}_{321}\text{Au}_{84}$ and $\text{Pt}_{394}\text{Au}_{96}$).

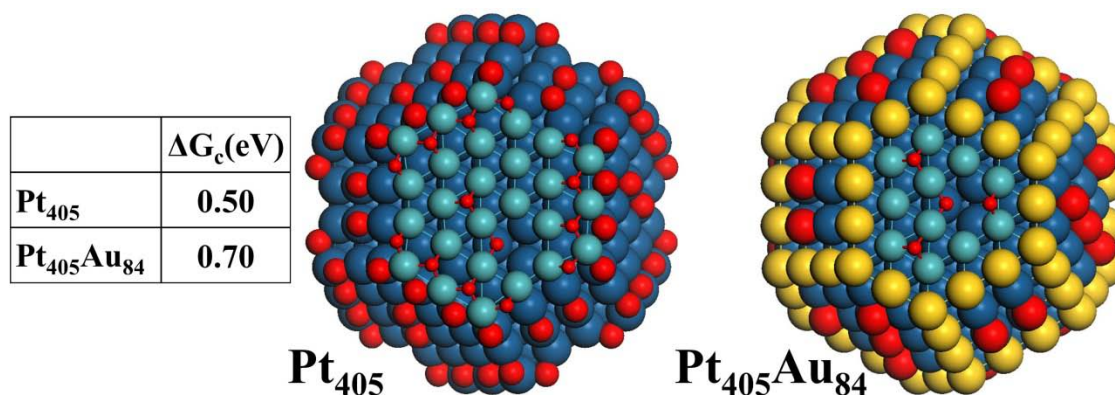


Fig. S8 Illustration of the structures for the surface vacancy phases of Pt_{405} and corresponding Au-framed Pt nanoparticle ($\text{Pt}_{321}\text{Au}_{84}$). The ΔG_c values (the reaction free energy change of $\text{O}_x/\text{Au}/\text{Pt}_{\text{nanoparticle}} \rightarrow \text{O}_x/\text{Au}/\square-\text{Pt}_{\text{nanoparticle}} + \text{Pt}^{2+} + 2e^-$, see the main text and Ref 22 for the calculation methods) of these two nanoparticles are listed in the insert table. Large blue ball and cyan ball: Pt atoms; large yellow ball: Au atoms; red ball: O atoms.

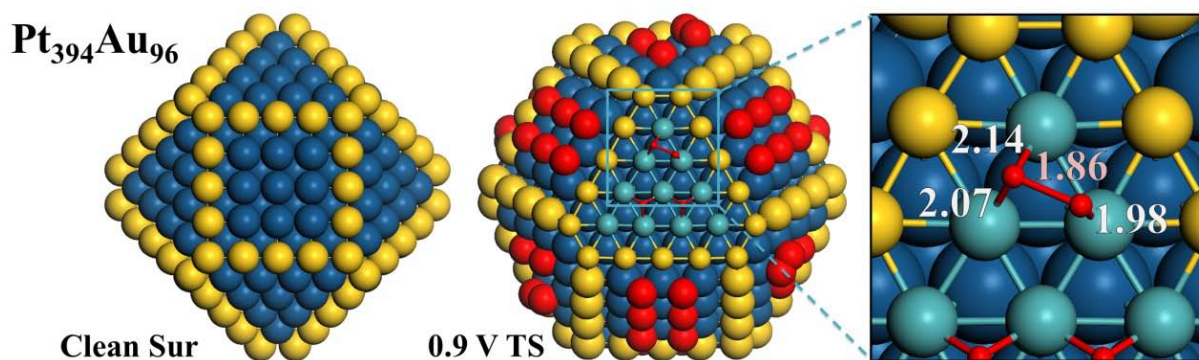


Fig. S9 The structure of $\text{Pt}_{394}\text{Au}_{96}$ nanoparticle and the located TS structures for O–O dissociation on $\text{Pt}_{394}\text{Au}_{96}$ at 0.9 V vs AHE. The nearby solvated proton [H_7O_3^+] that can stabilize the IS and TSs is not shown for clarity. Blue ball and cyan ball: Pt; yellow ball: Au; red ball: O.

Part V Other information

Table S2 The data of Fig. 1b (see the main text).

	Pt ₂₀₁	Pt ₂₈₈	Pt ₄₀₅	Pt ₄₉₀	Pt ₇₂₄	Pt ₁₄₀₀	Pt ₄₀₇₀	Pt ₅₃₂₄
D₍₁₁₁₎ (nm)	1.38	1.61	1.83	2.07	2.53	3.22	4.83	5.28
N_{terrace}/N_{particle}	0.31	0.31	0.30	0.27	0.25	0.24	0.20	0.19
N_{edge}/N_{particle}	0.30	0.25	0.21	0.20	0.17	0.11	0.05	0.05
N_{eff}/N_{particle}	0.04	0.06	0.07	0.07	0.05	0.04	0.03	0.03
PZC (V)	0.15	0.18	0.19	0.21	0.23	0.27	/	/
d_{Pt-Pt} (Å)[*]	2.812	2.815	2.817	2.817	2.819	2.823	/	/
d_{Pt-Pt}^{0.9V} (Å)^{**}	2.887	2.887	2.876	2.855	2.847	2.835	/	/
d_{Pt-O}^{0.9V} (Å)^{**}	2.042	2.024	2.025	2.001	1.977	1.986	/	/

* $d_{\text{Pt-Pt}}$ is the average Pt-Pt bond length in clean Pt nanoparticles.

** $d_{\text{Pt-Pt}}^{0.9\text{V}}$ and $d_{\text{Pt-O}}$ are the average Pt-Pt and Pt-O bond length in O covered Pt nanoparticles at 0.9V, respectively.

Part VI Our Procedure for Calculating Electrochemical Reaction

To study an electrochemical reaction under a constant potential as that encountered in experiment, we did a series of calculations with different surface charges for both the IS and the TS, e.g. generally from $-1|e|$ to $1|e|$ with every $0.1|e|$ increment. The reaction barrier can then be obtained for each fixed charge condition (the constant-charge condition). Next, we need to link the computed surface charge with the electrochemical potential and finally obtain the barrier at the concerned potential condition. Using DFT/CM-MPB method, for each state, the surface charge added can be linearly related to the computed electrochemical potential, as shown in Fig. S8. For the nanoparticle systems, the difference of computed potential at the TS and the IS are generally negligible (eg. only 0.01 and 0.03 V for the O-O direct dissociation and O-OH dissociation on Pt₂₈₈, respectively). Therefore, we can directly utilize the calculated electrochemical potential at the IS as the potential for the reaction to occur. The accuracy of the calculated electrochemical potential from DFT/CM-MPB has been examined by benchmarking the calculated pzc of typical metal surfaces with the experimental data, see Table S3.

For reactions involving the releasing of proton and electron, the reaction energy can be computed by referencing to the normal hydrogen electrode (SHE) in a manner proposed by the Bockris⁹ and Nørskov group¹⁰. This is governed by $G_{\text{proton+electron}} = G(\frac{1}{2}\text{H}_2) - neU$ where e presents the transfer electron, n means the number of electrons, and U is the electrochemical potential vs SHE.

Table S3 The calculated workfunction (in vacuum) and pzc of metal surfaces

Metal	Φ/eV^*	pzc /V*	$E_{\text{solv}}/\text{eV}^a$
Au(111)	5.19 (5.47)	0.34 (0.47-0.58)	-0.029
Pt(111)	5.52 (5.93)	0.29 (0.2-0.4)	-0.071
Ir(111)	5.25 (5.76)	0.00 (0.01-0.13)	-0.067
Ag(111)	4.51 (4.74)	-0.39 (-0.45)	-0.015
Pd(111)	5.40 (5.6)	0.25 (0.20)	-0.049
Rh(111)	5.03 (4.98)	0.01 (0.05-0.12)	-0.038

*The data in parenthesis are the experimental values (taken from Ref.^{11,12} and references therein).

^a E_{solv} refers to the solvation energy per surface atom.

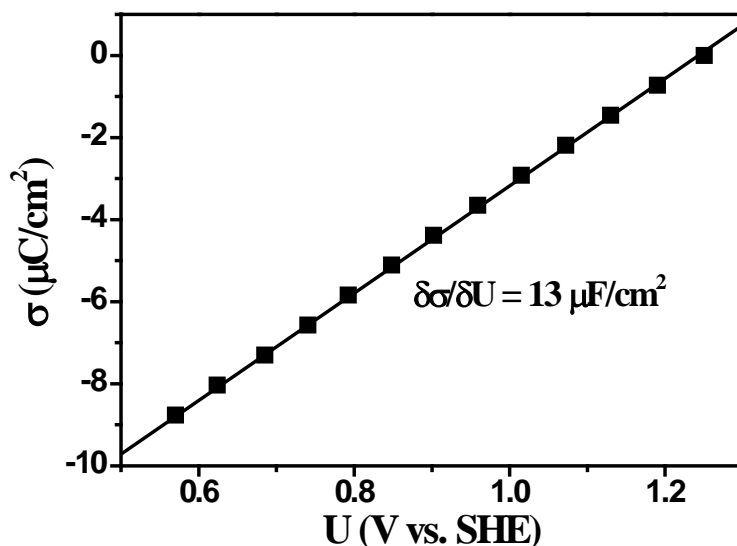


Fig. S10 The charge density ~ electrochemical potential curves for the initial state of an adsorbed O₂ reacting with solvated proton on Pt (111) with precovered 0.25 ML O.

References:

- 1 H. A. Hansen, J. Rossmeisl and J. K. Nørskov, *Phys. Chem. Chem. Phys.*, 2008, **10**, 3722-3730.
- 2 J. Rossmeisl, G. S. Karlberg, T. Jaramillo and J. K. Nørskov, *Faraday Discuss*, 2008, **140**, 337-346.
- 3 Y. H. Fang and Z. P. Liu, *J Phys Chem C*, 2010, **114**, 4057-4062.
- 4 Y. H. Fang and Z. P. Liu, *J. Phys. Chem. C*, 2009, **113**, 9765-9772.
- 5 R. Jinnouchi and A. B. Anderson, *Phys Rev B*, 2008, **77**, 18.
- 6 J. L. Fattebert and F. Gygi, *J Comput Chem*, 2002, **23**, 662-666.
- 7 Y. F. Li, Z. P. Liu, L. L. Liu and W. G. Gao, *J. Am. Chem. Soc.*, 2010, **132**, 13008-13015.
- 8 G. F. Wei and Z. P. Liu, *Energy & Environmental Science*, 2011, **4**, 1268-1272.
- 9 J. O. M. Bockris and S. U. M. Khan, Plenum Press, New York, 1993.
- 10 J. Rossmeisl, A. Logadottir and J. K. Nørskov, *Chem Phys*, 2005, **319**, 178-184.
- 11 D. R. LIDE, ed., *CRC Handbook of Chemistry and Physics*; , CRC press, 2003-2004.
- 12 S. Trasatti and E. Lust, in *The Potential of Zero Charge*, ed. A. E. B. White, J.O'M.; Conway, B. E., Kluwer Academic/Plenum Publishers, New York, Boston, Dordrecht, London, Moscow, 2002, vol. 33, pp. 1-303.